Attachment of Gold Nanograins onto Colloidal Magnetite Nanocrystals

Daniela Caruntu, Brian L. Cushing, Gabriel Caruntu,* and Charles J. O'Connor*

Advanced Materials Research Institute, University of New Orleans, New Orleans, Louisiana 70148-2820

Received February 6, 2005. Revised Manuscript Received April 25, 2005

The successful attachment of 2−3 nm gold particles to ∼10 nm Fe_3O_4 nanocrystals through a simple, two-step chemically controlled procedure is reported. The surface of individual, relatively monodisperse, Fe_3O_4 nanospheres forming a stable colloidal methanolic solution is coated with an amino-terminated silane, peptized to induce positive charges on the particles' surfaces and then treated with a colloidal solution of negatively charged Au nanoparticles. A detailed investigation by transmission electron microscopy, X-ray diffraction, UV−vis, inductively coupled plasma, and superconducting quantum interference device magnetometry was performed in order to elucidate the morphology and properties of the nanocomposites. Due to their low concentration and small size of the attached Au particles, the optical properties are not observable in the case of the Fe_3O_4/Au nanocomposites. Additionally, the colloidal Fe_3O_4/Au nanocomposites are highly stable against separation and exhibit magnetic properties similar to those of the parent Fe_3O_4 nanocrystals. These novel nanoarchitectures open up new opportunities for the use of magnetite nanoparticles for in-vivo biomedical applications through chemical bonding of bioactive molecules to the attached Au nanoparticles.

In the past few years, magnetite nanoparticles have become increasingly important for cutting-edge applications in biomedicine due to both their biocompatibility and attractive magnetic properties.[1] Super-paramagnetic magnetite nanocrystals possess high magnetic susceptibility, low remanence, low coercivity, and high saturation magnetization, making them ideal candidates for applications in magnetic resonance imaging (MRI), cancer/HIV diagnosis, magnetically controlled drug delivery, biological separation, enzyme and protein immobilization, magnetic cell sorting, RNA and DNA purification, retinal detachment therapy, biosensors, and magnetocytolysis.[2−7] Additionally, although nanocrystalline Fe_3O_4 presents a lower saturation magnetization than its metallic congeners, it exhibits a much higher chemical stability against oxidation, which enables magnetite nanocrystals to be easily dispersed in blood and directed to a specific target upon applying an external magnetic field.

For high-performance applications, magnetite nanoparticles are required to possess a narrow size distribution, smooth surface, a uniform spherical shape, and the ability to form colloidal suspensions in physiological fluids. This last condition has proven to be a critical shortcoming for practical applications because magnetic particles have the tendency to cluster and precipitate, which drastically reduces their efficiency. Advanced manipulation of magnetite nanoparticles for in-vivo diagnostic tests necessitates magnetic nanoparticles conjugated with bioactive molecules such as antibodies, nucleic acids, lipids, peptides, enzymes, proteins, or DNA. Biomolecule immobilization often requires chemical modification of the surface by complicated synthetic procedures.[8] This could be greatly simplified by coating magnetite nanoparticles with metallic nanoshells. Gold represents an excellent candidate by virtue of its easy reductive preparation, high chemical stability, biocompatibility, and its affinity for binding to amine/thiol terminal groups of organic molecules.[9] Ideally, gold nanoshells should be thin enough to induce minimal alteration of the magnetic properties of the magnetite core. Several recent papers have reported the synthesis of core−shell Fe_3O_4@Au nanocomposites, but, in most cases, the coating of individual magnetite nanoparticles and the tunability of the shell thickness still remain unresolved.[10,11]

Here, we report a facile, highly reproductive two-step synthetic process enabling the attachment of 2−3 nm gold clusters onto (3-aminopropyl)triethoxysilane (APTES)-coated Fe_3O_4 nanoparticles obtained by functionalization of Fe_3O_4 particles with a mean diameter of 10.4 nm. This work

* To whom correspondence should be addressed. Telephone: (504) 280-6846. Fax: (504) 280-3185. E-mails: (G.C.) gcaruntu@uno.edu; (C.J.O'C.) coconnor@uno.edu.

(1) Mornet, S.; Vasseur, S.; Grasset, F.; Duguet, E. *J. Mater. Chem.* **2004**, *14*, 2161.
(2) Tartaj, P.; Morales, M. P.; Veintemillas-Verdaguer, S.; Gonzales-Carreno, T.; Serna, C. J. *J. Phys. D: Appl. Phys.* **2003**, *36*, R182.
(3) Kim, D. K.; Mikhaylova, M.; Zhang, Y.; Muhammed, M. *Chem. Mater.* **2003**, *15*, 1617.
(4) Mykhaylyk, O.; Cherchenko, A.; Ilkin, A.; Dudchenko, N.; Ruditsa, V.; Novoseletz, M.; Zozulya, Y. *J. Magn. Magn. Mater.* **2001**, *225*, 241.
(5) Knauth, M.; Egelhof, T.; Roth, S. U.; Wirtz, C. R.; Sartor, K. *Am. J. Neuroradiol.* **2001**, *22*, 99.
(6) Bergemann, C.; Muller-Schulte, D.; Oster, J.; Brassard, L.; Lubbe, A. S. *J. Magn. Magn. Mater.* **1999**, *194*, 45−52.
(7) Roullin, V. G.; Deverre, J. R.; Lemaire, L.; Hindre, F.; Julienne, M. C. V.; Vienet, R.; Benoit, J. P. *Eur. J. Pharm. Biopharm.* **2002**, *53*, 293.
(8) Landfester, K.; Ramirez, L. P. *J. Phys.: Condens. Matter* **2003**, *15*, S1345.
(9) Daniel, M.-C.; Astruc, D. *Chem. Rev.* **2004**, *104*, 293.
(10) Lyon, J. L.; Flemming, D. A.; Stone, M. B.; Schiffer, P.; Williams, M. E. *Nano Lett.* **2004**, *4*, 719.
(11) Mikhaylova, M.; Kim, D. K.; Bobrysheva, N.; Osmolowsky, M.; Semenov, V.; Tsakalatos, T.; Muhammed, M. *Langmuir* **2004**, *20*, 2472.

10.1021/cm050280n CCC: $30.25
Published on Web 05/28/2005

exploits the strong ability of gold metal to bind covalently to the lone pair of the terminal $-NH_2$ groups of organic entities, interactions that can be further enhanced by mutually attractive electrostatic interactions when the two components are oppositely charged. Though such a method has proven to be simple, inexpensive, and versatile, little emphasis has been placed on the design of nanocomposite architectures with tailorable properties and complex functionalities by the immobilization of metal nanoclusters onto different kinds of nanoparticles. Previous attempts include the work of Halas and co-workers, who designed a bottom-up approach for the preparation of core−shell SiO_2@Au nanocomposites by the sequential attachment of gold nanoparticles to the surface-modified SiO_2 nanocrystals.[12] The growth of these attached gold nanoparticles by the subsequent reduction of Au^{3+} in aqueous solutions finally results in the formation of a continuous thin gold layer at the surface of the SiO_2 nanocrystals. Recently, Sun and co-workers have reported the preparation of dumbbell-like bifunctional Au−Fe_3O_4 nanocomposites by the thermal decomposition of $Fe(CO)_5$ at 300 °C in the presence of Au nanoparticles dispersed into a noncoordinating solvent under inert atmosphere.[13] Additionally, all of the other related papers cover extensively the immobilization of noble metals onto different bare/surface-functionalized inorganic nanocrystals having applications in optical devices and catalysis.[14−17] Though Fe_3O_4/Au nanocomposites represent a relevant system with superior magnetic properties and potential widespread use in biomagnetics, such composites have been largely ignored in favor of Fe_3O_4@Au core−shell nanostructures.

Highly crystalline magnetite nanoparticles were prepared by the hydrolysis of chelated iron alkoxide complexes at elevated temperature in solutions of diethylene glycol (DEG) and *N*-methyldiethanolamine (NMDEA; 3:1, w/w). In a typical experiment, a 4 mmol amount of $FeCl_2 \cdot 4H_2O$ and 8 mmol of $FeCl_3 \cdot 6H_2O$ were dissolved in 120 g of diethylene glycol (DEG) in a Schlenk flask under protection with argon. When the salts were completely dissolved, 40 g of NMDEA was added and the solution immediately turned from yellow-brown to deep brown-green. The resulting solution was allowed to stir for 1 h. Separately, 32 mmol of NaOH was dissolved in 60 g of DEG and then mixed with 20 g of NMDEA. The solution of NaOH was added to the solution of metal chlorides while being stirred at room temperature, causing an immediate color change from deep brown-green to deep green. After 3 h, the temperature of the solution was raised during 1.5 h to 210 °C and then kept constant for 3 h in the temperature range of 210−220 °C. After cooling the reaction mixture to room temperature, the obtained black solid was isolated by centrifugation, washed with a mixture of ethanol and ethyl acetate (1:1, v/v) three times, and then dispersed in methanol.

As demonstrated in our previous paper, the surfaces of the as-prepared Fe_3O_4 nanocrystals are passivated by the molecules of the adsorbed solvents (DEG and NMDEA), which bind the superficial Fe ions via the ligand's lone pairs, thus rendering the nanoparticles soluble in polar solvents (water, methanol, and ethanol).[18] Furthermore, organic molecules such as DEG and NMDEA are known to possess the ability to act as tridentate ligands for the transition metal ions, forming two-ring, chelating complexes.[19] Although the mechanistic pathway of the bonding of these organic molecules to the oxide nanocrystals' surface is not completely elucidated, it is likely that when adsorbed on the surface, these molecules partially use their chelating properties and leave some of the hydroxo groups available for further derivatization.

For the synthesis of the nanocomposite material, we used colloidal solutions of Fe_3O_4 nanoparticles in methanol that exhibit long sedimentation times, being stable against agglomeration for several months. The first step of the synthetic process consists of functionalizing the Fe_3O_4 nanocrystals with APTES. Recently, two independent papers reported the functionalization with APTES of magnetite nanoparticles obtained by coprecipitation of Fe^{2+} and Fe^{3+} salts in aqueous solution.[20,21] The authors demonstrated that the hydroxy groups on the magnetite surface react with the ethoxy groups of the APTES molecules with the formation of Si−O bonds and leave the terminal $-NH_2$ groups available for enzyme immobilization.[21] However, in both cases the APTES functionalization of individual Fe_3O_4 nanoparticles is hampered by the relatively high agglomeration level of the coprecipitated nanopowders. In contrast to the coprecipitation procedure, our nonaqueous synthetic approach allows the two chelating solvents (DEG and NMDEA) to protect the nanocrystals against agglomeration, induce their solubility in polar solvents, and favor the reactions at the nanocrystal's surface, thus rendering them more suitable for individual functionalization with organic molecules. For the functionalization of Fe_3O_4 nanocrystals with APTES, 2 mL of ferrofluid (∼10 mg of Fe_3O_4/mL of methanol solution) was diluted to 50 mL with absolute ethanol and sonicated for 2−3 min. The resulting colloidal solution was transferred to a three-neck flask equipped with a condenser, a thermometer, and a heating mantle. Then, 180 μL of APTES was injected into the flask, and the mixture was vigorously stirred at room temperature for about 1 h and then heated to reflux for 2 h under protection with argon. After the mixture was cooled to room temperature, the solid product was magnetically separated, washed with ethanol five times, and then redispersed in 10 mL of ethanol by sonicating for 10 min. To induce positive charges at the surface of the APTES-

(12) Westcott, S. L.; Oldenburg, S. J.; Lee, T. R.; Hallas, N. J. *Langmuir* **1998**, *14*, 5396.
(13) Yu, H.; Chen, M.; Rice, P. M.; Wang, S. X.; White, R. L.; Sun, S. *Nano Lett.* **2005**, *5*, 379.
(14) Serp, P.; Feurer, R.; Kihn, Y.; Kalck, P.; Faria, J. L.; Figueiredo, J. L. *J. Mater. Chem.* **2001**, *11*, 1080.
(15) Zhang, F.; Guan, N.; Li, Y.; Zhang, X.; Chen, J.; Zhang, H. *Langmuir* **2003**, *19*, 8230.
(16) Mandal, S.; Roy, D.; Chaudhari, R. V.; Sastry, M. *Chem. Mater.* **2004**, *16*, 3714.
(17) Zhang, F.; Chen, J.; Zhang, X.; Gao, W.; Jin, R.; Guan, N.; Li, Y. *Langmuir*, **2004**, *20*, 9329.
(18) Caruntu, D.; Caruntu, G.; Chen, Y.; Goloverda, G.; O'Connor C. J.; Kolesnichenko, V. *Chem. Mater.* **2004**, *16*, 5527.
(19) Greenwood, N. N.; Earnshaw, A. *Chemistry of Elements*, 2nd ed.; Butterworth & Heinneman: Oxford, U.K., 1997; p 906.
(20) Ming; M.; Zhang, Y.; Yu, W.; Shen, H.; Zhang, H.; Gu, N. *Colloids Surf., A* **2003**, *212*, 219.
(21) Shen, X. C.; Fang, X. Z.; Zhou, Y. H.; Liang H. *Chem. Lett.* **2004**, *33*, 1468.

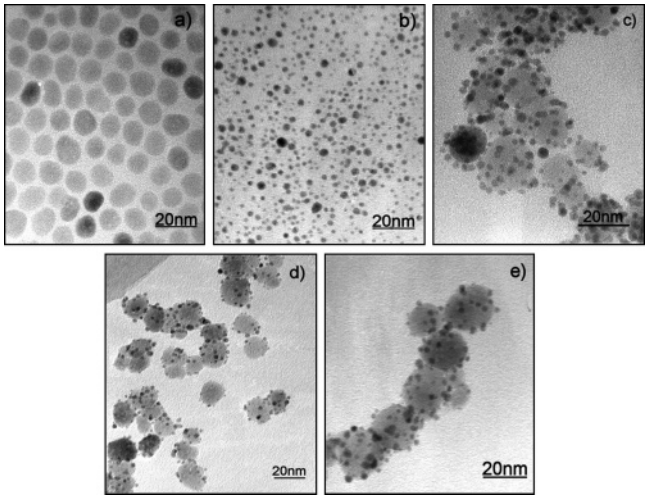

Figure 1. Typical TEM images of the as-prepared Fe_3O_4 nanoparticles obtained from a mixture of DEG and NMDEA (3:1, w/w) (a), the colloidal Au particles (b), the freshly prepared Fe_3O_4/Au nanocomposite material (c), and the Fe_3O_4/Au nanocomposite material aged for 2 and 5 months (d, e) and sonicated for 60 min.

coated Fe_3O_4 nanocrystals, 10 drops of HNO_3 solution (prepared by mixing 0.05 mL of 6 M HNO_3 with 20 mL of ethanol) was introduced into the ethanolic dispersion of APTES-coated Fe_3O_4 and then stirred for 4 h. The second step in the synthesis of Fe_3O_4/Au nanocomposites is the attachment of 2−3 nm gold particles onto APTES-coated Fe_3O_4 nanoparticles. Negatively charged gold nanoparticles were prepared by a modification of the method of Duff et al.[22] In a typical experiment, 5 mL of 1 M NaOH was diluted with 18 mL of distilled water and then mixed with 10 mL of tetrakis(hydroxymethyl)phosphonium chloride (THPC; 0.67 mmol) solution. The THPC stock solution was prepared separately by diluting 0.6 mL of 80% THPC (3.375 mmol) aqueous solution with 50 mL of deionized water. The resulting solution containing the reducing agent was allowed to stir for 5 min. Then, 20 mL of 1% $HAuCl_4$ solution was added slowly to the above mixture kept under vigorous stirring to yield a deep red-brown solution, indicating the formation of Au nanoparticles. The resulting colloidal gold solution was stirred continuously for 10 min. Once prepared, the negatively charged gold nanoparticles contained in the colloidal solution were attached to the surface of aminosilane-coated Fe_3O_4 nanocrystals. Thus, 30 mL of colloidal gold solution was introduced into a round-bottom flask containing 10 mL of the ethanolic dispersion of amine-functionalized Fe_3O_4 nanoparticles, and the mixture was stirred overnight at room temperature. The solid product was collected by magnetic separation, washed in sequence with ethanol and distilled water five times to remove the excess of gold particles, and then redispersed in ethanol by sonication. From these solutions, samples for XRD and magnetic measurements were prepared by drying the solid material at room temperature under flowing nitrogen. Figure 1 shows the transmission electron microscope (TEM) images of (a) the Fe_3O_4 nanoparticles obtained from a mixture of DEG and NMDEA (3:1, w/w), (b) the colloidal THPC-coated gold particles, (c) the as-prepared Fe_3O_4/Au nanocomposite material, and (d and e) the ethanolic solution of Fe_3O_4/Au nanocomposites aged for 2 and 5 months, respectively, and sonicated for 60 min.

(22) Duff, D. G.; Baiker, A.; Edwards, P. P. *Langmuir* **1993**, *9*, 2301.

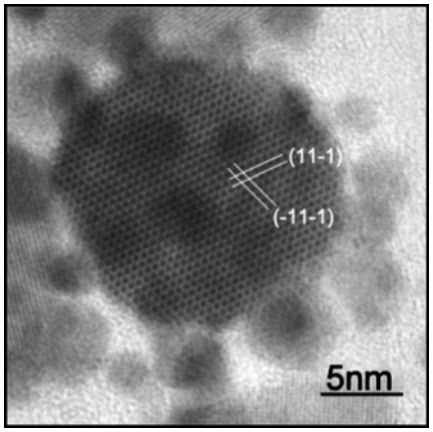

Figure 2. Representative high-resolution TEM image of a typical Au-decorated Fe_3O_4 nanocrystal viewed along [011] zone axis.

The micrographs clearly show that the attachment of gold nanoparticles onto individual Fe_3O_4 nanocrystals was successful. However, as seen in Figure 1c, some agglomeration of the Fe_3O_4/Au nanocomposites is observed, but the initial spherical Fe_3O_4 nanoparticles can still be individually distinguished. We observe that the parent Fe_3O_4 nanoparticles are slightly aggregated, most of them appearing as discrete units which exhibit individual spherical shapes. At the same time, the Fe_3O_4/Au nanosized composites show a remarkable resistance to sonication; most of the gold particles are still attached onto the surface of Fe_3O_4 nanocrystals even after sonication for 1 h. While the mechanism of attachment is still unclear, TEM data suggest that the bonding of colloidal gold nanoparticles to the surface of APTES-modified Fe_3O_4 nanoparticles' is relatively strong and probably not strictly electrostatic. From the HRTEM image (Figure 2), one can easily identify the 2−3 nm gold particles (smaller, darker dots) attached to spherical Fe_3O_4 nanocrystals.

Because of their small size, the lattice fringes of the 2−3 nm attached gold particles cannot be distinguished, whereas for the larger Fe_3O_4 nanocrystals, lattice fringes corresponding to the $(11\bar{1})$ and $(\bar{1}1\bar{1})$ atomic planes are easily identified. The interplanar distance calculated from the corresponding HRTEM image is 4.85 Å, whereas the zone axis is [011]. Although the number of gold particles attached to each individual Fe_3O_4 nanocrystal varies between neighboring particles, no uncoated magnetite nanocrystals were observed. From the XRD pattern in Figure 3, all reflections can be ascribed to nanocrystalline Fe_3O_4, whereas the most intense reflection of Au, specifically the (111), is identified by a broad, low-intensity peak centered at 38° 2θ.

The absence of individual peaks corresponding to gold is likely due to the low concentration of gold in the composite material, the very small size of the gold particles, and/or their amorphous nature resulting from reduction of the $AuCl_4^-$ ions in the presence of THPC. The small amount of gold attached to the magnetite nanoparticles was further confirmed by inductively coupled plasma (ICP) emission spectrophotometry, which gave a weight percentage of 43.67% Fe_3O_4, 8.31% Si, and 48.01% Au, respectively.

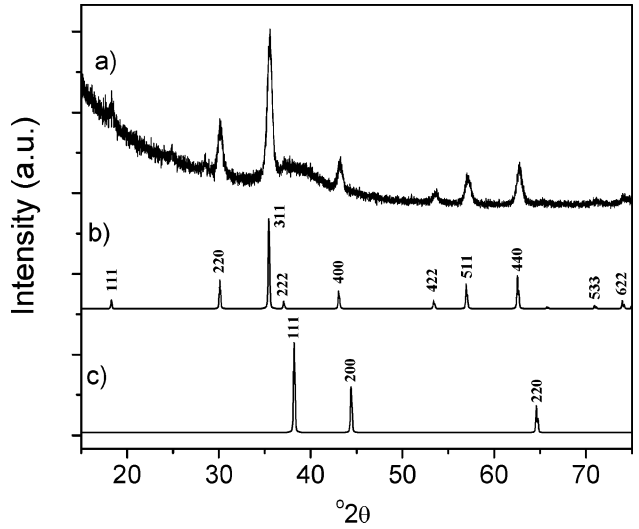

Figure 3. XRD pattern of the Fe_3O_4/Au nanocomposite (a) with simulated reference patterns of magnetite (b) and gold (c).

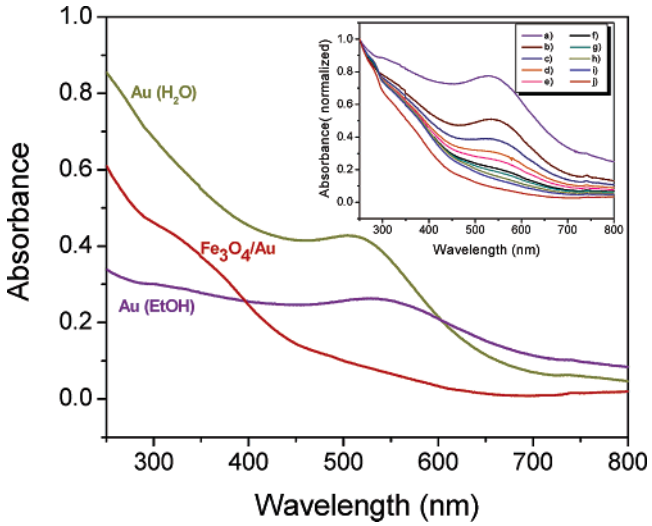

Figure 4. UV−vis spectra of Fe_3O_4/Au nanocomposites. The inset represents the UV−vis spectra of a physical mixture of colloidal 3−6 nm Au nanoparticles and 10.2 nm Fe_3O_4.

Figure 4 illustrates the UV−vis spectra of the freshly prepared gold nanoparticles dispersed in water and ethanol, as well as the spectra of an ethanolic solution of Fe_3O_4/Au nanocomposites. When dispersed in water, the as-prepared colloidal gold nanoparticles exhibit a plasmon peak at 515 nm that is shifted to 537 nm when the gold nanoparticles are dispersed in ethanol. The characteristic gold plasmon peak was not observed in the Fe_3O_4/Au nanocomposite. We hypothesize that the absence of the plasmon peak is due to both the low concentration of gold particles in the composite material and their small size.

The influence of the gold concentration on the intensity of the gold plasmon peak was investigated by recording the UV−vis spectra of a physical mixture of ethanolic dispersions of Fe_3O_4 nanocrystals and gold nanoparticles (inset of Figure 4). The intensity of the plasmon absorption peak at 537 nm (typical for THPC gold nanoparticles dispersed in ethanol) decreases monotonically as the concentration of gold in the physical mixture decreases. Curves a−j differ by 10% increments of the Au concentration from 100% (curve a) to 0% (curve j). Interestingly, we observed that the immobilization of the gold nanoparticles onto the Fe_3O_4 nanocrystals is size-selective. Careful examination of TEM micrographs reveals that the as-prepared gold nanoparticles exhibit a relatively broad size distribution, with sizes ranging between 2 and 7 nm in diameter, whereas the gold nanoparticles immobilized onto the Fe_3O_4 nanocrystals are significantly smaller, ranging between 1 and 4 nm (Figure 5). Fitting the size distribution profiles with a Gaussian function gives an average particle size of 3.4 nm (SD = 0.7) for the as-prepared Au nanoparticles and 2.5 nm (SD = 0.6) for the gold in the composite material. This strongly suggests that size effects play an important role in the formation of the Fe_3O_4/Au nanocomposites and that the ∼10 nm APTES-coated Fe_3O_4 nanocrystals preferentially bind smaller gold nanoparticles. Consequently, the plasmon peak observed in the UV−vis spectra of both the aqueous and ethanolic gold colloids is attributed to the larger gold nanoparticles, whereas the Fe_3O_4/Au nanocomposites produce a plasmonless UV−vis spectrum. This observation agrees with the suggestion of other authors that for a collection of very small gold nanoparticles (d < 3 nm), finite-size effects become significant, thus suppressing the characteristic plasmon peak in the corresponding UV−vis spectrum (since the main contribution to the plasmon peak mainly originates from the surface scattering of the conduction electrons, its intensity follows a 1/r dependence with the size of the particle).[23]

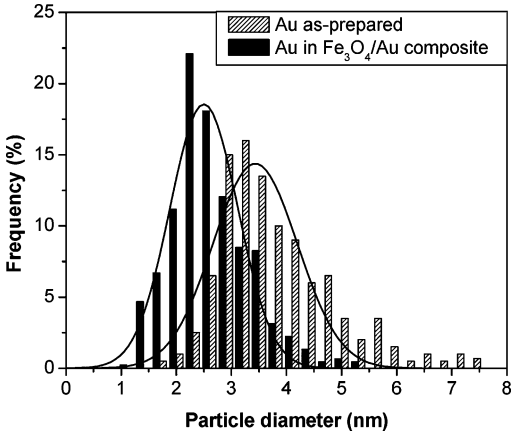

Figure 5. Size distribution plots of as-prepared Au nanoparticles and Au nanoparticles immobilized onto 10 nm Fe_3O_4 nanocrystals. Solid lines represent the fitted Gaussian distribution functions.

The ZFC/FC curves of the gold-decorated Fe_3O_4 nanoparticles and the bare Fe_3O_4 nanoparticles measured in a field of 100 Oe on a superconducting quantum interference device (SQUID) magnetometer are plotted in Figure 6. The absence of a well-defined maximum in the ZFC curve indicates that both the bare 10 nm Fe_3O_4 nanoparticles and Fe_3O_4/Au nanocomposites exhibit blocking temperatures (T_B) above room temperature. Furthermore, no visible difference between the two curves was detected upon immobilization of 2−3 nm gold particles onto the ∼10 nm Fe_3O_4 particles. It is known that the maximum of the ZFC curve for a collection of superparamagnetic noninteracting single-domain nanoparticles is dependent on the size of nanocrystals and their degree of clustering, as well as on the mutual dipolar

(23) Vogel, W.; Duff, D. G.; Baiker, A. *Langmuir* **1995**, *11*, 401.

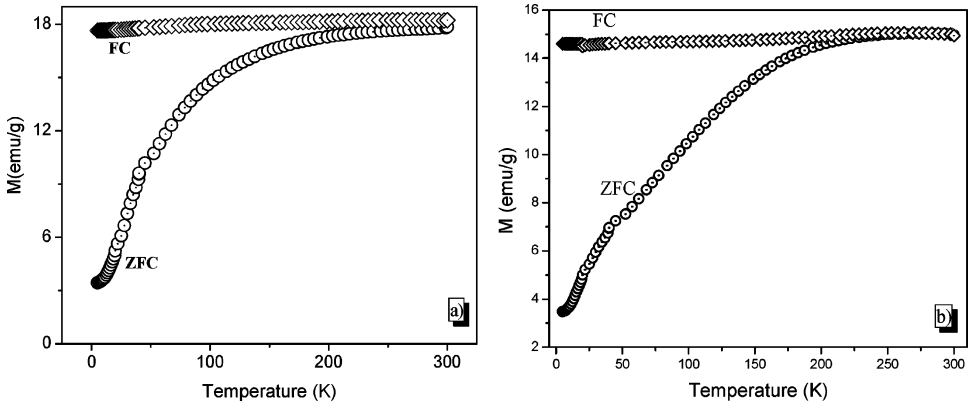

Figure 6. ZFC/FC curves of bare Fe_3O_4 nanoparticles (a) and Fe_3O_4/Au nanocomposites (b).

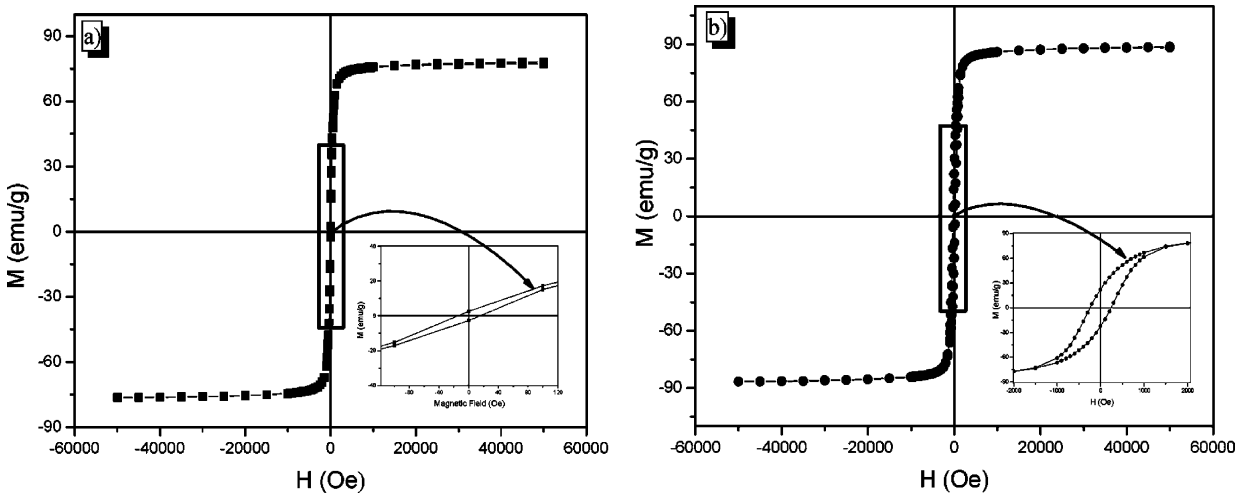

Figure 7. Hysteresis loops of Fe_3O_4/Au nanoclusters recorded at 300 (a) and 5 K (b).

interactions between them.[24] However, in the case of Fe_3O_4/Au nanocomposites, the ZFC and FC curves diverge at $T = 198$ K, which is a much lower temperature than the $T = 228$ K observed in the case of the bare Fe_3O_4 nanoparticles. This could be associated with a lowering of the anisotropic energy barrier for the Fe_3O_4/Au nanocomposites with respect to that of the bare Fe_3O_4 nanocrystals.

The hysteresis loops of the Fe_3O_4/Au nanocomposites, recorded at 300 and 5 K, are represented in Figure 7. As expected from the shape of the ZFC/FC curves, the Fe_3O_4/Au exhibits a hysteretic behavior at both temperatures. The coercivity (H_c) and squareness (SQ) are found to increase from $H_c = 15$ Oe and $SQ = M_r/M_s = 0.034$ at 300 K to $H_c = 246$ Oe and $SQ = 0.25$ at 5 K, respectively.

The magnetic data show that the room-temperature saturation magnetization (M_s) of the 10 nm Fe_3O_4 particles is 83.5 emu/g, close to the value of 92 emu/g reported for bulk material.[25] The saturation magnetization of the Fe_3O_4/Au nanocomposites was found to be 78 emu/g at 300 K and 89 emu/g at 5 K, respectively. The values of M_s for the Fe_3O_4/Au nanocomposites were normalized to the weight of the magnetic core as determined by ICP measurements. Moreover, the M_s of Fe_3O_4/Au nanocomposites is very close to the value of 80 emu/g reported for 3−14 nm Au−Fe_3O_4 dumbbell nanoparticles synthesized by Sun and co-workers[13] and undoubtedly show that that the M_s of Fe_3O_4 nanoparticles is minimally influenced by the immobilization of gold nanoparticles on their surfaces.

In summary, we describe a simple and feasible sequential approach to immobilize 2−3 nm gold particles onto the chemically modified surface of 10 nm Fe_3O_4 particles prepared from a nonaqueous, homogeneous solution of diethylene glycol and *N*-methyldiethanolamine (3:1, w/w). The process is size-selective, and in the case of Fe_3O_4/Au nanocomposites, both the low concentration and the small size of the gold particles immobilized on the ∼10 nm Fe_3O_4 nanoparticles obscure the gold plasmon peak. The attached gold particles provide chemically active sites on the surface of the magnetite nanocrystals, enabling their potential derivatization with different multifunctional organic molecules. This effective approach can be readily extended to the immobilization of other noble metals onto the chemically modified surface of magnetite nanocrystals, also opening up new potential avenues for the functionalization of these nanoensembles and their further manipulation in specific biochemical applications.

Acknowledgment. This work has been supported by DARPA through Grant HR0011-04-C-0068. The authors thank Prof. Weilie Zhou and Dr. Yuxi Chen for assistance with the TEM studies.

CM050280N

(24) Hou, Y.; Yu, J.; Gao, S. *J. Mater. Chem.* **2003**, *13*, 1983.
(25) Cornell, R. M.; Schwertmann, U. *The Iron Oxides: Structure, Properties, Reactions, Occurrence and Uses*; VCH: New York, 1996.